

# Multiscale Finite Elements for Linear Elasticity: Oscillatory Boundary Conditions

Marco Buck<sup>1</sup>, Oleg Iliev<sup>1</sup>, and Heiko Andrá<sup>1</sup>

## 1 Introduction

Multiscale finite element methods (MsFEMs) have been widely used when solving elliptic PDEs with highly oscillating coefficients on multiple scales. Beyond their application in the upscaling framework [7, 8, 9, 3], they are often utilized for the construction of robust coarse spaces in the context of two-level overlapping domain decomposition preconditioners.

In [4, 2, 15] coarse basis functions are constructed by solving local generalized eigenvalue problems. The scalar multiscale finite element basis is used as a partition of unity to setup the spectral problems and allows the dimension of the resulting coarse space to be sufficiently low. The method guarantees robustness for various elliptic PDEs with respect to arbitrary coefficient variations. Another recent approach where generalized eigenvalue problems are solved in overlapping regions of local subdomains is presented in [13]. It provides applications to isotropic linear elasticity problems with robustness properties similar to them in [4, 2, 15].

For scalar elliptic PDEs it is shown in [5, 6] that oscillatory multiscale finite element coarse spaces ensure robustness for a large class of coefficient variations. This includes variations in the interior of coarse elements, but allows coefficient jumps also across coarse element boundaries when high contrast regions can be characterized as a union of disjoint islands.

A first application of the multiscale finite element method with (vector-valued) linear boundary conditions to linear elasticity (see also the adaptive method in [11]) is given in [1]. If material jumps occur only in the interior of coarse grid elements, uniform condition number bounds which do not depend on the contrast in the Young's modulus are obtained. However, the method fails to be robust when stiff inclusions touch coarse element boundaries. This motivates the construction of boundary conditions for the multiscale finite element basis which adapt to the heterogeneities in the PDE coefficients.

The outline of the paper is as follows. In Section 2 we state the equations of linear elasticity and briefly describe their discretization with vector-valued piecewise linear finite elements. The abstract two-level additive Schwarz method is summarized in Section 3. Section 4 contains the detailed introduction of the oscillatory multiscale finite element basis. Numerical results are presented in Section 5 and final conclusions are given in Section 6.

---

<sup>1</sup> Fraunhofer Institute for Industrial Mathematics (ITWM), Fraunhofer-Platz 1, 67663 Kaiserslautern, Germany, e-mail: {Buck, Iliev, Andrae}@itwm.fraunhofer.de

## 2 Finite Element Discretization in Linear Elasticity

Let  $\Omega \subset \mathbb{R}^d$  be a bounded, polyhedral ( $d = 3$ ) or polygonal ( $d = 2$ ) Lipschitz domain. The displacement field  $u = (u_1, \dots, u_d)^\top$  of a solid body in  $\Omega$ , deformed under the action of a volume force  $f$  and a traction force  $t$ , is governed by the mixed BVP

$$\begin{aligned} -\operatorname{div} \sigma(u) &= f \text{ in } \Omega, \\ \sigma(u) &= C : \varepsilon(u) \text{ in } \Omega, \end{aligned} \quad (1)$$

where  $\sigma$  is the stress tensor,  $\varepsilon$  is the strain tensor and  $C(x)$  is the fourth order elasticity tensor. The system in equation (1) is subject to the boundary conditions

$$u = 0 \text{ on } \Gamma_D, \quad \sigma(u)n = t \text{ on } \Gamma_N,$$

where  $n$  is the unit outer normal vector on  $\partial\Omega = \overline{\Gamma_D} \cup \Gamma_N$  with  $\operatorname{meas}(\Gamma_D) > 0$ . Let  $\mathcal{T}_h$  be a tetrahedral ( $d = 3$ ) or triangular ( $d = 2$ ) mesh and let  $\Sigma_h(\bar{\Omega})$  denote the set of vertices in  $\bar{\Omega}$ . We introduce a finite element discretization  $u_h$  of displacements  $u$  on the space  $\mathcal{V}^h := \operatorname{span}\{\varphi_k^{j,h} : \bar{\Omega} \rightarrow \mathbb{R}^d, x^j \in \Sigma_h(\bar{\Omega}), k = 1, \dots, d\}$  of continuous piecewise linear vector-valued functions on  $\mathcal{T}_h$ . Assuming enough regularity, the discretization leads to a symmetric positive definite linear system  $A\mathbf{u} = \mathbf{f}$  (see e.g. [10] for more details).

## 3 Overlapping Domain Decomposition Preconditioners

We are interested in constructing two-level overlapping domain decomposition preconditioners for the linear system which are robust w.r.t. mesh parameters and variations in the PDE coefficients. They combine local solves on overlapping subdomains  $\{\Omega_i, i = 1, \dots, N\}$  (with overlap-width  $\delta > 0$ ) and a global solve on a coarse grid  $\mathcal{T}_H$ . Let  $\mathcal{V}^0 \subset \mathcal{V}_0^h$  be a coarse space defined on  $\mathcal{T}_H$  and let  $\mathcal{V}^i = \mathcal{V}^h(\Omega_i)$  be the space of vector-valued linear basis functions on  $\mathcal{T}_h$  which are supported in  $\Omega_i, i = 1, \dots, N$ . The action of the two-level additive Schwarz preconditioner is defined implicitly by

$$M_{\text{AS}}^{-1} = R_0^\top A_0^{-1} R_0 + \sum_{i=1}^N R_i^\top A_i^{-1} R_i,$$

where  $R_i, i = 0, \dots, N$  is the restriction operator from  $\mathcal{V}^h$  to  $\mathcal{V}^i$  and  $A_i = R_i A R_i^\top$  is the corresponding submatrix of  $A$  (cf. [14]). We assume here that  $\mathcal{T}_H$  also consists of tetrahedra ( $d = 3$ ) or triangles ( $d = 2$ ), each of which consists of a union of fine elements  $\tau \in \mathcal{T}_h$ . For any  $D \subset \bar{\Omega}$ , we denote by  $\Sigma_H(D)$  the set of nodes of  $\mathcal{T}_H$  in  $D$  and  $\mathcal{N}_H(D)$  is the corresponding index-set of coarse nodes.

## 4 Multiscale Finite Elements for Linear Elasticity

Multiscale basis functions with oscillatory boundary conditions are introduced for scalar elliptic PDEs in [7] to reflect the heterogeneities in the PDE coefficients also across coarse element boundaries. In this section we present the extension to linear elasticity. We define the multiscale basis and introduce suitable coordinate transformations that allow the derivation of the equations which govern the boundary data of the oscillatory multiscale basis on general meshes. On composites with isotropic constituents, we present the construction in detail. We denote by  $\bar{\omega}_p := \{T \in \mathcal{T}_H : p \in \mathcal{N}_H(T)\}$  the union of coarse elements which share the node  $x^p \in \Sigma_H(\bar{\Omega})$ . For any  $p \in \mathcal{N}_H(\bar{\Omega})$  and  $m \in \{1, \dots, d\}$ , the oscillatory multiscale basis function  $\mathcal{V}^h \ni \phi_m^{p, \text{MsO}} : \omega_p \rightarrow \mathbb{R}^d$ , is defined such that for  $T \subset \bar{\omega}_p$ ,

$$\begin{aligned} \operatorname{div}(\mathbf{C} : \varepsilon(\phi_m^{p, \text{MsO}})) &= 0 && \text{in } T, \\ \phi_m^{p, \text{MsO}} &= \eta_m^{p, T} && \text{on } \partial T, \end{aligned} \quad (2)$$

where the oscillatory boundary data  $\eta_m^{p, T} : \partial T \rightarrow \mathbb{R}^d$  are continuous and compatible, i.e.  $\eta_m^{p, T} = \eta_m^{p, T'}$  on  $\partial T \cap \partial T' \subset \bar{\Omega}$  for  $T, T' \in \mathcal{T}_H$ . We impose the vector-valued nodal constraints

$$\eta_{mk}^{p, T}(x^q) = \delta_{pq} \delta_{mk}, \quad x^q \in \mathcal{N}_H(T), \quad k \in \{1, \dots, d\} \quad (3)$$

and show how  $\eta_m^{p, T} = (\eta_{m1}^{p, T}, \dots, \eta_{md}^{p, T})^\top$  is derived in Section 4.2 and 4.3.

### 4.1 Coordinate Transformation

The boundary data  $\eta_m^{p, T}$  in equation (2) are extracted by solving a restricted version of the PDE (1) to the coarse element boundary which implies that  $\phi_m^{p, \text{MsO}}|_{\partial T}$  is independent of the coordinate in the direction normal to  $\partial T$ . To make the construction applicable to edges and faces of  $T \in \mathcal{T}_H$  which are not aligned with or perpendicular to one of the coordinate axis, we apply a suitable coordinate transformation of the Cartesian coordinate system with basis  $\{e^1, \dots, e^d\}$  to a (right handed) coordinate system with orthonormal basis  $\{\hat{e}^1, \dots, \hat{e}^d\}$ . W.l.o.g., for any

edge  $\mathcal{E}$ : we introduce the rotated coordinate system such that  $\hat{e}^1$  is parallel to  $\mathcal{E}$   
 face  $\mathcal{F}$ : we introduce the rotated coordinate system such that the normal vector  $n$  on  $\mathcal{F}$  is parallel to one of the coordinate axis, i.e.  $\hat{e}^3 = n$ .

Let  $\hat{x}_1, \dots, \hat{x}_d$  be the coordinates of  $x = (x_1, \dots, x_d)^\top$  w.r.t. the transformed basis. The coordinate transformation can be described by a linear map  $\Theta : T \rightarrow \mathbb{R}^d$ ,  $\hat{x} = \Theta x$  with  $\theta_{ij} = \hat{e}^i \cdot e^j$ ,  $1 \leq i, j \leq d$ . The elasticity coefficients of the stiffness tensor  $\hat{\mathbf{C}}$  transform under the rotation of the coordinate system to  $\hat{c}_{ijkl} = \sum_{p,q,r,s=1}^d \theta_{ip} \theta_{jq} \theta_{kr} \theta_{ls} c_{pqrs}$  (cf. [12]).

## 4.2 Equations Governing the Oscillatory Boundary Data

Using the rotated coordinate system in Section 4.1, we derive the reduced problems on a face  $\mathcal{F}$  of  $T \in \mathcal{T}_H$  for the system of anisotropic linear elasticity. The components of the elasticity operator in equation (1) read

$$\sum_{j=1}^d \partial_j \sigma_{ij}(u) = \sum_{j=1}^d \partial_j \left( \sum_{k,l=1}^d c_{ijkl} \varepsilon_{kl}(u) \right). \quad (4)$$

Forcing that  $\hat{\phi}_m^{p,\text{MsO}} = \hat{\eta}_m^{p,T}(\hat{x}_1, \dots, \hat{x}_{d-1})$  is independent of  $\hat{x}_d$  on  $\mathcal{F}$  and using the symmetry  $\hat{c}_{ijkl} = \hat{c}_{ijlk}$  of the stiffness tensor, we obtain by using  $\hat{\varepsilon}_{kl}(\hat{u}) = \frac{1}{2}(\hat{\partial}_k \hat{u}_l + \hat{\partial}_l \hat{u}_k)$  in the rotated coordinate system

$$\begin{aligned} \sum_{j=1}^d \hat{\partial}_j \hat{\sigma}_{ij}(\hat{\eta}_m^{p,T}) &= \sum_{j=1}^{d-1} \hat{\partial}_j \left( \sum_{k,l=1}^d \hat{c}_{ijkl} \hat{\varepsilon}_{kl}(\hat{\eta}_m^{p,T}) \right) \\ &= \sum_{j=1}^{d-1} \hat{\partial}_j \left( \sum_{k,l=1}^{d-1} \hat{c}_{ijkl} \hat{\varepsilon}_{kl}(\hat{\eta}_m^{p,T}) + 2 \sum_{k=1}^{d-1} \hat{c}_{ijkd} \hat{\varepsilon}_{kd}(\hat{\eta}_m^{p,T}) \right) \\ &= \sum_{j=1}^{d-1} \hat{\partial}_j \left( \sum_{k,l=1}^{d-1} \hat{c}_{ijkl} \hat{\varepsilon}_{kl}(\hat{\eta}_m^{p,T}) \right) \end{aligned} \quad (5)$$

$$+ \sum_{j=1}^{d-1} \hat{\partial}_j \left( \sum_{k=1}^{d-1} \hat{c}_{ijkd} \hat{\partial}_k \hat{\eta}_{md}^{p,T} \right). \quad (6)$$

While equation (5) affects exclusively the first two components of  $\hat{\eta}_m^{p,T}$ , equation (6) acts only on the third component of the oscillatory boundary data on  $\mathcal{F}$ . For an anisotropic stiffness tensor, a reduced system needs to be solved on  $\mathcal{F}$  in which the three components of  $\hat{\eta}_{m2}^{p,T}$  are coupled. Having a deeper look at the entries of the stiffness tensor, the systems in (5) and (6) are fully decoupled for an orthotropic material whose symmetry axes are normal to  $\hat{e}^1, \dots, \hat{e}^d$ . Particularly, the components  $\hat{\eta}_{m1}^{p,T}$  and  $\hat{\eta}_{m2}^{p,T}$  on  $\mathcal{F}$  are then governed by a 2D system of linear elasticity (see (5)), while the component  $\hat{\eta}_{md}^{p,T}$  normal to  $\mathcal{F}$  is governed by a scalar second order elliptic PDE (see (6)). Analogously, on an edge  $\mathcal{E}$ , we can deduce that the boundary data  $\hat{\eta}_m^{p,T}(\hat{x}_1)$  are governed by scalar second order PDEs in each particular component which may, again, be coupled in the anisotropic case.

## 4.3 Oscillatory Boundary Conditions for Isotropic Linear Elasticity

Given the formulation of the reduced problems in a suitable coordinate system, we summarize the procedure of computing boundary data  $\eta_m^{p,T}$  on the faces and edges of  $T$ , assuming that the stiffness tensor is isotropic. Its components are given by

$c_{ijkl} = \lambda \delta_{ij} \delta_{kl} + \mu (\delta_{ik} \delta_{jl} + \delta_{il} \delta_{jk})$ , where  $\mu > 0$  and  $\lambda \geq -\frac{2}{3}\mu$  are the Lamé coefficients of the material (see e.g. [10]) which we assume here to be piecewise constant in  $\tau \in \mathcal{T}_h$ . Note that the material coefficients are not uniquely determined on  $\partial T$ , a proper averaging (e.g. by taking their maximum values) in the adjacent elements  $\tau \in \mathcal{T}_h$  is required.

From (5) and (6), together with  $\hat{\eta}_m^{p,T} = \hat{\eta}_m^{p,T}(\hat{x}_1)$  along the edge  $\mathcal{E}$ , the reduced problem in rotated coordinates reads

$$\begin{aligned} \hat{\partial}_1 \left( (\lambda + 2\mu) \hat{\partial}_1 \hat{\eta}_{m1}^{p,T} \right) &= 0 \text{ on } \mathcal{E}, \\ \hat{\partial}_1 \left( \mu \hat{\partial}_1 \hat{\eta}_{mk}^{p,T} \right) &= 0 \text{ on } \mathcal{E}, \quad k = 2, 3. \end{aligned} \quad (7)$$

It needs to be equipped with the boundary conditions defined in (3). Let us assume that  $\mathcal{E} = \mathcal{E}_{p_1 p_2}$  connects the two nodes  $x^{p_1} = x^p, x^{p_2} \in \Sigma_H(\bar{\Omega})$ , then we impose

$$\begin{aligned} \hat{\eta}_m^{p,T}(\hat{x}^{p_1}) &= \Theta e^m, \\ \hat{\eta}_m^{p,T}(\hat{x}^{p_2}) &= (0, 0, 0)^\top. \end{aligned} \quad (8)$$

In order to grasp immediately that the boundary data on a face  $\mathcal{F}$  are governed by a reduced elasticity system in the first two components and a scalar elliptic problem in the component normal to  $\mathcal{F}$ , we state the equations governing the reduced problem under the assumption that  $\lambda$  and  $\mu$  are piecewise constant on  $\mathcal{F}$ . This allows to simplify the notation of the reduced system without affecting its weak formulation. According to equation (5) and (6), the reduced system reads

$$\begin{aligned} \mu (\hat{\partial}_{11} \hat{\eta}_{m1}^{p,T} + \hat{\partial}_{22} \hat{\eta}_{m1}^{p,T}) + (\lambda + \mu) (\hat{\partial}_{11} \hat{\eta}_{m1}^{p,T} + \hat{\partial}_{12} \hat{\eta}_{m2}^{p,T}) &= 0 \text{ a.e. on } \mathcal{F}, \\ \mu (\hat{\partial}_{11} \hat{\eta}_{m2}^{p,T} + \hat{\partial}_{22} \hat{\eta}_{m2}^{p,T}) + (\lambda + \mu) (\hat{\partial}_{21} \hat{\eta}_{m1}^{p,T} + \hat{\partial}_{22} \hat{\eta}_{m2}^{p,T}) &= 0 \text{ a.e. on } \mathcal{F}, \\ \mu (\hat{\partial}_{11} \hat{\eta}_{m3}^{p,T} + \hat{\partial}_{22} \hat{\eta}_{m3}^{p,T}) &= 0 \text{ a.e. on } \mathcal{F}. \end{aligned} \quad (9)$$

Let  $\mathcal{F} = \mathcal{F}_{p_1 p_2 p_3}$  contain the coarse nodes  $x^{p_1}, x^{p_2}$  and  $x^{p_3}$ . Then the three edges  $\mathcal{E}_{p_1 p_2}, \mathcal{E}_{p_1 p_3}$  and  $\mathcal{E}_{p_2 p_3}$  form the 2D boundary of the face  $\mathcal{F}$ . The system in (9) is subject to the boundary conditions

$$\hat{\eta}_m^{p,\mathcal{F}}|_{\mathcal{E}_{p_k p_l}} = \hat{\eta}_m^{p,\mathcal{E}_{p_k p_l}} \quad 1 \leq k < l \leq 3,$$

where  $\hat{\eta}_m^{p,\mathcal{E}_{p_k p_l}}$  is the solution of the BVP in (7) and (8) on the edge  $\mathcal{E}_{p_k p_l}$  in the coordinate system w.r.t.  $\mathcal{F}$  and  $\hat{\eta}_m^{p,\mathcal{D}}$  denotes the restriction of  $\hat{\eta}_m^{p,T}$  to  $\mathcal{D} \subset \partial T$ . Note that the rotated coordinate systems differ for any face and edge. Once the boundary data are computed on an edge or a face, they should be transformed to the original coordinate system.

#### 4.4 Properties of the Oscillatory Multiscale Basis

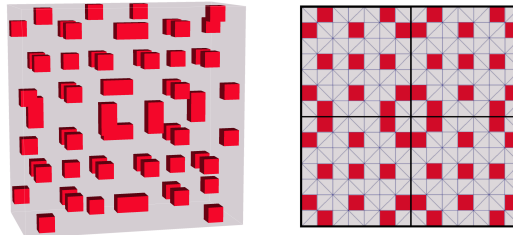
As shown in [1], the multiscale basis with vector-valued linear boundary data (*MsL*) recovers all rigid body modes. If no material jumps occur on the boundaries of coarse elements, it can be shown that  $\phi_m^{p,MsO} = \phi_m^{p,MsL}$ . Prescribing homogeneous material parameters, both multiscale bases coincide with the vector-valued linear coarse basis. Furthermore, the construction of the oscillatory multiscale basis guarantees that the rigid body translations are contained in the coarse space. In general, not all the rigid body rotations are preserved exactly on the coarse element boundaries. The complexity of computing  $\phi_m^{p,MsO}$  is of the same asymptotic order  $O(d(\frac{H}{h})^d)$  as for  $\phi_m^{p,MsL}$ , with a small additional cost that is one order of  $\frac{H}{h}$  cheaper.

### 5 Numerical Results

In this section we present numerical examples on a binary composite. We apply different coarsening strategies for the two-level additive Schwarz preconditioner, including a vector-valued linear coarse space as well as multiscale coarse spaces with linear and oscillatory boundary conditions. We perform the simulations on a domain  $\bar{\Omega} = [0, 1] \times [0, 1] \times [0, L], L > 0$ , using regular fine and coarse triangular meshes  $\mathcal{T}_h$  and  $\mathcal{T}_H$  of equal structure with uniform mesh size  $h$  and  $H$ , respectively. Both meshes are constructed from an initial voxel geometry by decomposing each voxel into five tetrahedra. In the experiments we show condition numbers as well as iteration numbers of the PCG algorithm. The stopping criterion is set to reduce the preconditioned initial residual by 6 orders of magnitude.

The medium consists of an isotropic matrix material with coefficients ( $\mu_{\text{mat}} = 1$ ,  $\lambda_{\text{mat}} = 1$ ) and contains inclusions ( $\mu_{\text{inc}}, \lambda_{\text{inc}}$ ) which are positioned equally in each coarse block of size  $H \times H \times H$  as shown in Fig. 1. The distribution of the inclusions as well as the boundaries of the coarse tetrahedra are shown in more detail in Fig. 2. At each slice in the plane normal to  $X_1$  and  $X_2$  the position of the inclusions above and below this level are indicated in dark and shaded red, respectively. Each inclusion touches or crosses coarse element boundaries while one inclusion in the center is isolated in the interior of a coarse element. Table 1 shows the condition

**Fig. 1** Binary composite; matrix material (grey) and inclusions (red); discretization in  $14 \times 14 \times 7$  voxels (left); 2D-projection onto the  $(X_1, X_2)$ -plane with position of the inclusion (right); each coarse block is decomposed in five tetrahedra;



and iteration numbers for the three coarsening strategies under the variation of the material contrast  $\Delta_E := \mu_{\text{inc}}/\mu_{\text{mat}} = \lambda_{\text{inc}}/\lambda_{\text{mat}}$ . For  $\Delta_E > 1$ , condition and iteration numbers for vector-valued linear and multiscale coarse space with linear boundary conditions grow with the contrast in the material coefficients, where the latter does not perform noticeably better than the linear coarse space. The multiscale coarse basis functions with oscillatory boundary conditions are bounded in energy and show coefficient-independent bounds of the condition number. For  $\Delta_E < 1$ , each coarse space performs well.

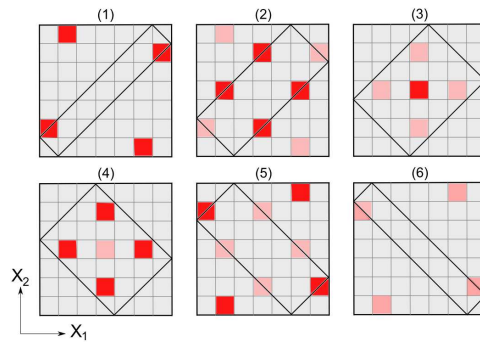
**Table 1** Condition numbers  $\kappa$  and iteration numbers (#it) of precond. matrix for  $H = 7h$ ,  $\delta = 2h$

$\Delta_E$	Lin	MsL	MsO
$10^{-9}$	26 (28)	26 (28)	26 (28)
$10^{-6}$	26 (28)	26 (28)	26 (28)
$10^{-3}$	26 (28)	26 (28)	26 (28)
$10^0$	25 (27)	25 (27)	25 (27)
$10^3$	426 (91)	233 (76)	25 (27)
$10^6$	965 (102)	955 (104)	25 (27)
$10^9$	970 (102)	955 (104)	25 (27)

## 6 Conclusions

In this study, we extended the oscillatory multiscale finite element method as introduced in [7] to the PDE system of anisotropic linear elasticity. We derived the reduced system which governs the oscillatory boundary data in a general setting which allows their construction on triangular, tetrahedral, quadrilateral and hexahedral coarse meshes. We applied the coarse basis in the context of two-level additive Schwarz domain decomposition preconditioners. Numerical results are presented on a tetrahedral mesh for isotropic composites where inclusions touch the coarse

**Fig. 2** 2D-slices (at  $X_3 = lh$ ,  $l \in \{1, \dots, 6\}$ ) of a coarse block of  $7 \times 7 \times 7$  voxels of the medium in Fig. 1; boundaries of coarse tetrahedral elements (black), matrix material (grey) and  $1 \times 1 \times 1$  inclusions (red); inclusions touch the slice from below (shaded red) or top (dark red); inclusions touch coarse element boundaries



element boundaries. We observed condition number bounds of the preconditioned linear system which are independent of the contrast in the Young's modulus in the inclusions.

It is easy to verify (see e.g. [1]) that the computation of a multiscale finite element basis is more costly on quadrilateral and hexahedral coarse meshes than on their triangular and tetrahedral counterparts (by a factor of  $\frac{4}{3}$  in 2D and a factor of 2 in 3D). However, we may point out that, especially for applications in three spatial dimensions, using hexahedral coarse meshes may be beneficial for the robustness of the overall method as it reduces the amount of element boundaries which are introduced when tetrahedral coarse meshes are used.

**Acknowledgements** The authors would like to thank Prof. Yalchin Efendiev and Prof. Victor Calo for fruitful discussions and their valuable comments on the subject of this manuscript.

## References

1. Buck, M., Iliev, O., Andrä, H.: Multiscale finite element coarse spaces for the application to linear elasticity. *Cent. Eur. J. Math.* **11**(4), 680–701 (2013)
2. Efendiev, Y., Galvis, J., Lazarov, R., Willems, J.: Robust domain decomposition preconditioners for abstract symmetric positive definite bilinear forms. *Math. Model. Numer. Anal.* **46**, 1175–1199 (2012)
3. Efendiev, Y., Hou, T.: *Multiscale finite element methods, theory and applications*, 4 edn. (2009)
4. Galvis, J., Efendiev, Y.: Domain decomposition preconditioners for multiscale flows in high-contrast media: reduced dimension coarse spaces. *Multiscale Model. Simul.* **8**(5), 1621–1644 (2010)
5. Graham, I.G., Lechner, P.O., Scheichl, R.: Domain decomposition for multiscale PDEs. *Numer. Math.* **106**, 589–626 (2007)
6. Graham, I.G., Scheichl, R.: Robust domain decomposition algorithms for multiscale PDEs. *Numer. Methods Partial Differ. Equ.* **23**, 859–878 (2007)
7. Hou, T.Y., Wu, X.H.: A multiscale finite element method for elliptic problems in composite materials and porous media. *J. Comput. Phys.* **134**, 169–189 (1997)
8. Hou, T.Y., Wu, X.H.: A multiscale finite element method for PDEs with oscillatory coefficients. *Note Num. Fl.* **70**, 58–69 (1999)
9. Hou, T.Y., Wu, X.H., Cai, Z.: Convergence of a multiscale finite element method for elliptic problems with rapidly oscillating coefficients. *Math. Comp.* **68**, 913–943 (1999)
10. Hughes, T.J.R.: *The finite element method: Linear static and dynamic finite element analysis*. Prentice-Hall, Inc. (1987)
11. Millward, R.: *A new adaptive multiscale finite element method with applications to high contrast interface problems*. Ph.D. thesis, University of Bath (2011)
12. Norris, A.: Euler-rodriques and Cayley formulas for rotation of elasticity tensors. *Math. Mech. Solids* **13**, 465–498 (2008)
13. Spillane, N., Dolean, V., Hauret, P., Nataf, F., Pechstein, C., Scheichl, R.: Abstract robust coarse spaces for systems of PDEs via generalized eigenproblems in the overlaps. Tech. Rep. 2011-07, University of Linz, Institute of Computational Mathematics (2011)
14. Toselli, A., Widlund, O.: *Domain decomposition methods, algorithms and theory*. Springer (2005)
15. Willems, J.: *Robust multilevel methods for general symmetric positive definite operators*. Tech. Rep. 2012-06, RICAM Institute for Computational and Applied Mathematics (2012)